國立嘉義大學生命科學院

學生學術研究成果優良海報評選獲獎名單

時間:108 年 6 月 5 日

碩博士組

名次	獲獎人姓名	指導教師
食品科學系		
第一名	陳怡文	呂英震
第二名	馬雅均	呂英震
第三名	許　強	吳思敬
生物資源學系		
第一名	陳毓蓁	劉以誠
第二名	林唐禕	陳宣汶
第三名	黃志銓	劉以誠
生化科技學系		
第一名	胡愷真	張心怡
第二名	陳冠宇	陳瑞傑
第三名	邵楚雯	張心怡
微生物免疫與生物藥學系		
第一名	彭俊鈺	陳俊憲
第二名	王蕙心	王紹鴻
第三名	王心妤	翁博群

生化科技學系

國立嘉義大學
National Chiayi University

Analysis of the Active Constituents and Evaluation of the Biological Effects of Ultrasonic extract of *Eleutherococcus senticosus* roots

Kai-Chen Hu[1] and Hsin-I Chang*[1]

[1] Department of Biochemical Science and Technology, National Chia Yi University, No 300, Syuefu Rd, Chiayi City 60004, Taiwan

ABSTRACT

Eleutherococcus senticosus (ES) is widely distributed in the northeastern region of China, Korea, and Japan, and the far-eastern region of Russia. In the past, ES was commonly used as traditional Chinese herbal medicine for the treatment of weakness, debility, lassitude, anorexia and insomnia. Recently, a great number of pharmacological studies have reported that the root extract of ES has anti-inflammatory, anti-fatigue, anti-depressive, and anti-oxidant effects against oxidative damage. Therefore, we suggested that the extract of ES root may have the beneficial potential in skin due to the highly biological activities.

In this study, we extracted ES root with water and 15% ethanol solution by ultrasonic extraction equipment and measured the biological activities including antioxidant, anti-inflammatory and anti-skin aging effects. After the measurement of anti-oxidant activity in different solvent extracts of ES root, 15% ethanol extract of ES root was chosen for the further analysis. Our results presented that 15% ethanol extract of ES root dose-dependently decreased LPS-induced nitrite production (NO) and prostaglandin E_2 (PGE_2) expression in RAW264.7 macrophages as compared with control. In Hs68 human dermal fibroblasts, the ethanol extract of ES root increased the protein expression of collagen and elastin in a dose-dependent manner. Moreover, we used H_2O_2 to induce the oxidative damage in Hs68 fibroblasts and found that ES extract could suppress the SA-β-Gal expression and intracellular ROS production in H_2O_2-stimulated Hs68 fibroblasts. Continually, ES extract can promote wound healing in Hs68 fibroblasts through the enhancement of cell migration. We also measured the bioactive compounds in ethanol extract of ES root, including the total phenolic acid, flavonoid and triterpenoid contents. The results displayed that the ethanol extract of ES root contained 7.2μg phenolic acid /mg、5.5μg flavonoid /mg and 4.8 ± 0.1μg triterpenoid /mg. In order to identify the compounds in the ethanol extract of ES root, we used HPLC for chemical analysis and found that the main bioactive constituents were identified as eleutheroside B, eleutheroside E and chlorogenic acids.

Taken together, these results demonstrated that the ethanol extract of ES root was considered as beneficial functional material to prevent oxidative stress-induced premature skin aging. Therefore, ES root has great potential in cosmetic, food or other bio-industries due to its beneficial effects.

RESULTS

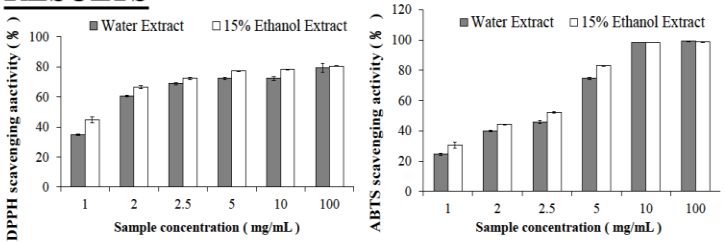

Figure. 1 Antioxidant activities of ES root extracts

Content (μg/mg)	Water Extract	15% Ethanol Extract
Total phenolic content	5.6 ± 0.1	7.2
Flavonoid content	3.5 ± 0.1	5.5
Triterpenoid content	2.1 ± 0.1	4.8 ± 0.1

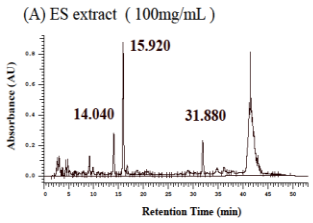

Figure. 2 Various antioxidant compounds in ES root extracts

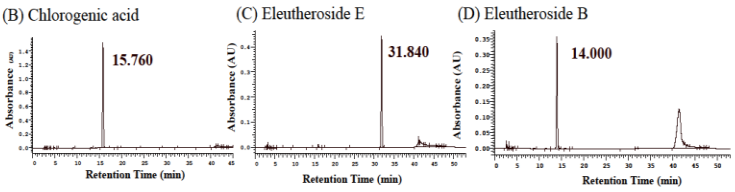

Figure. 3 HPLC chromatograms of 15% ethanol extract of ES root

CONCLUSIONS

- we found that 15% ethanol extract of *Eleutherococcus senticosus* root had higher anti-oxidant activity and which may be related to higher content of phenolic acids, flavonoids and titerpenoids in comparison with water extract. We identified the major bioactive compounds in ES extract, including eleutheroside B, chlorogenic acid and eleutheroside E by HPLC.
- In vitro experiments, ES root extract showed the anti-inflammatory activity through the inhibition of NO and PGE_2 productions in LPS-stimulated RAW264.7 macrophages.
- For investigating ECM synthesis in dermis, ES root extract could increase collagen and elastin levels and facilitate wound healing in Hs68 human dermal fibroblasts.
- ES root extract can suppress hydrogen peroxide-induced intracellular ROS production, thereby significantly prevent against H_2O_2-induced premature senescence in Hs68 human dermal fibroblasts.

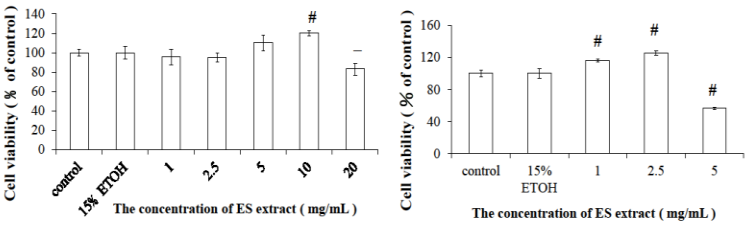

Figure. 4 The effect of ES root extracts on cell viability in RAW264.7 mouse macrophages and Hs68 human dermal fibroblasts

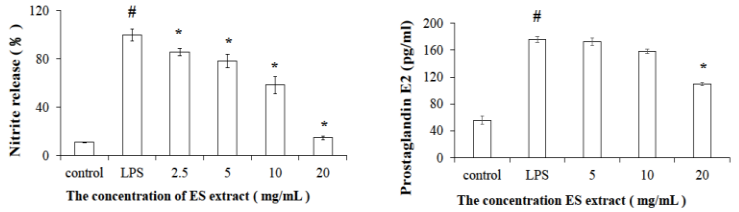

Figure. 5 The effect of ES root extracts on anti-inflammatory activity in LPS-stimulated RAW264.7 cells

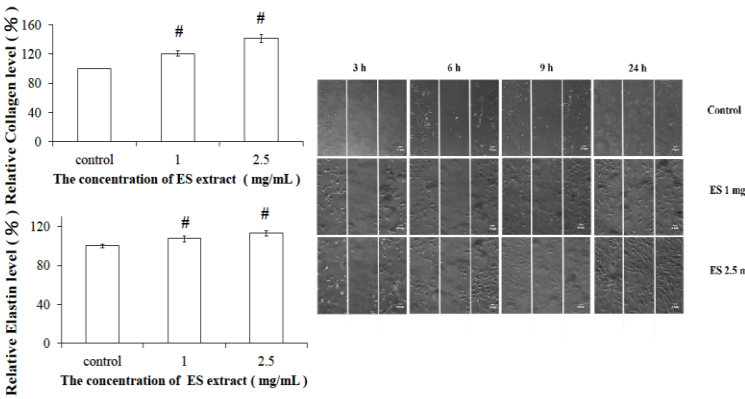

Figure. 6 The effect of ES root extract on the level of collagen and elastin expression, wound healing potential in Hs68 fibroblasts

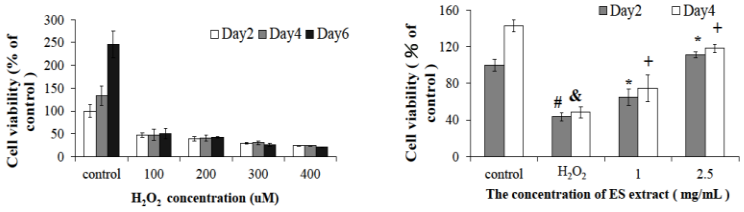

Figure. 7 Protective effect of ES root extracts on cell viability in H_2O_2-induced Hs68 fibroblasts

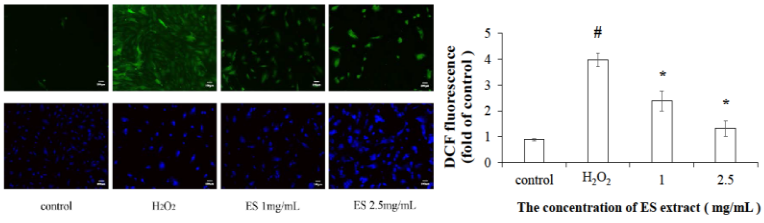

Figure. 8 Inhibitory effect of ES root extract on oxidative stress-induced intracellular ROS production in Hs68 fibroblasts

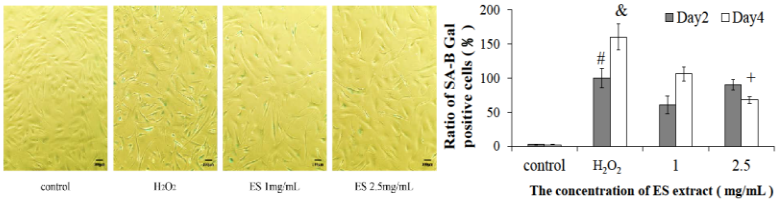

Figure. 9 Inhibitory effect of ES root extract on oxidative stress-induced senescence-associated β-galactosidase (SA-β-gal) activity in Hs68 fibroblasts

To explore the mechanisms of basic fibroblast growth factor on regulating doxorubicin resistance in human chondrosarcoma

Kuan-Yu Chen[1], Jui-Chieh Chen[1]
1.Department of Biochemical Science and Technology, National Chiayi University, Chiayi, Taiwan

Abstract

Chondrosarcomas are malignant cartilaginous neoplasms with diverse morphological features.They account for about 20% of all primary malignant tumors of the bone, which is generally relative resistance to conventional chemo- and radiotherapy. Doxrubicin(Dox) is currently used to treat a variety of cancer types. including chondrosarcomas. Due to lack of effective treatment for advanced chondrosarcoma, the clinical management of this disease is exceptionally challenging. Therefore, the novel therapeutic modalities are urgently needed. The tumor microenvironment, including cell-cell and cell-matrix interactions, may provide a survival advantage following initial drug exposure to promote drug resistance. We hypothesized that secreted factors present in the tumor microenvironment of chondrosarcoma is possible to drive Dox resistance. To evaluate whether Dox can alter the profile of secreted proteins in chondrosarcoma cells, we first used the antibody array to analyze the cell culture supernatant from Dox-treated and untreated cells.

Our results revealed that basic fibroblast growth factor (bFGF) exhibited the highest degree of secretion in Dox-treated cells. In addition, we also found that bFGF can promote the expression of XRCC5 (x-ray repair cross-complementing group 5) that is a key mediator of DNA repair for double-strand break. To further explore the relationship between bFGF and XRCC5 in Dox resistance, we established Dox-resistant chondrosarcoma cell lines. The results demonstrated that bFGF was highly expressed in Dox-resistant cells, and cells with high bFGF expression can maintain the amount of XRCC5 after Dox treatment. Moreover, we also used the knockdown technologies and pretreatment of exogenous recombinant bFGF to further verify the relationship between bFGF and XRCC5 in Dox resistance. These findings may provide rationale to combine Dox with blockade of bFGF-related pathways for the effective treatment of chondrosarcoma.

Results

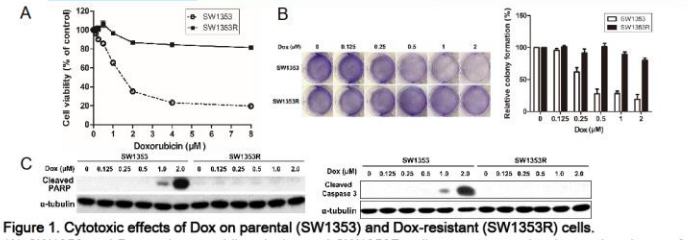

Figure 1. Cytotoxic effects of Dox on parental (SW1353) and Dox-resistant (SW1353R) cells.
(A) SW1353 and Dox-resistant subline designated SW1353R cells were exposed to increasing doses of doxorubicin for 24 h and assayed for survival by MTT assay. (B) The long-term effects of Dox were assessed by colony formation assay. A representative image shows that SW1353 cells formed fewer colonies compared to SW1353R cells. Lower panel is the result of densitometric data of the clonogenic growth of SW1353 and SW1353R cells. (C) Cells were treated with indicated concentration of Dox (0-2 μM) for 24 h and the expression levels of apoptosis-related proteins (cleaved PARP and cleaved caspase3) were examined by Western blot. α-Tubulin was used as a loading control.

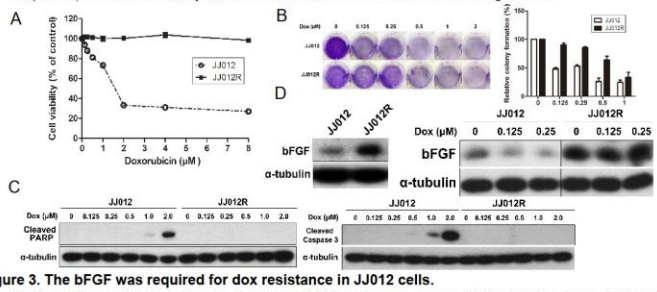

Figure 3. The bFGF was required for dox resistance in JJ012 cells.
(A) JJ012 and Dox-resistant subline designated JJ012R cells were exposed to increasing doses of doxorubicin for 24 h and assayed for survival by MTT assay. (B) The long-term effects of Dox were assessed by colony formation assay. A representative image shows that JJ012 cells formed fewer colonies compared to JJ012R cells. Right panel is the result of densitometric data of the clonogenic growth of JJ012 and JJ012R cells. (C) Cells were treated with indicated concentration of Dox (0-2 μM) for 24 h and the expression levels of apoptosis-related proteins (cleaved PARP and cleaved caspase3) were examined by Western blot. α-Tubulin was used as a loading control. (D) The bFGF protein expression levels in JJ012 and JJ012R cells were analyzed by Western blot. α-Tubulin was used as a loading control. Western blot shows dose-dependent effects of Dox on the expression of bFGF in JJ012 and JJ012R cells at indicated dose for 24 h. α-Tubulin was used as a loading control.

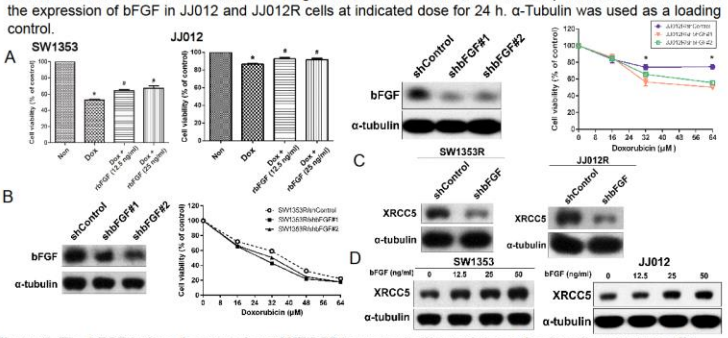

Figure 4. The bFGF induced expression of XRCC5 to promote dox resistance in chondrosarcoma cells.
(A) Cells were pretreated with rbFGF (12.5 ng/ml) and (25 ng/ml) for 4 h followed stimulation with 16 nM Dox for 48 h. Cell viability was examined by MTT assay. Results are expressed as mean ± SEM. * *P* < 0.05 compared with untreated group (Non) ; # P < 0.05 compared with Dox-treated group (left panel: SW1353; right panel: JJ012). (B) The protein levels of bFGF in shControl and shbFGF were examined by Western blot.α-Tubulin was used as a loading control. Cells were exposed to increasing concentrations of Dox for 24 h and subsequently evaluated by MTT assay.(down panel : SW1353R;up panel : JJ012R) The percentage of cell viability is shown relative to untreated controls.(C) The protein levels of XRCC5 in shControl and shbFGF were examined by Western blot.α-Tubulin was used as a loading control (left panel: SW1353R; right panel: JJ012R). (D) Cell were treated with different concentrations of bFGF (0-50 ng) for 24 h. The XRCC5 was analyzed by Western blot with specific antibodies.(left panel: SW1353; right panel: JJ012).

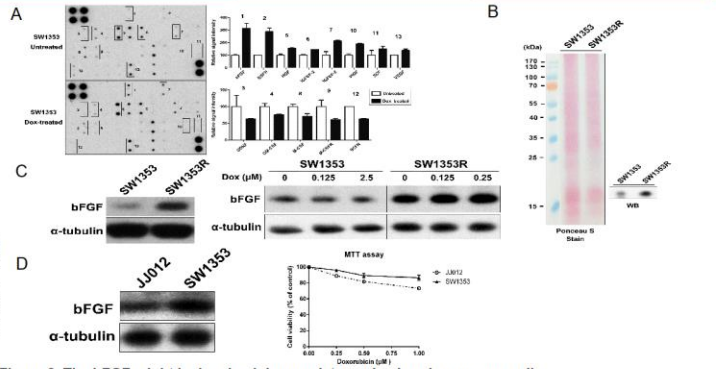

Figure 2. The bFGF might be involved drug resistance in chondrosarcoma cells.
(A) Human growth factor antibody array. Each antibody was spotted in duplicate. Results revealed a marked increase in the activation of bFGF. The marked molecules are significantly changed as indicated by numbers. Right panel is the result of densitometric data of the pair of duplicate spots representing each marked protein. (B) An equal volume of conditioned media (CM) from SW1353 and SW1353R cells was analyzed for secreted bFGF by Western blot. Loading quantities were shown on left side by Ponceau S staining. (C) The bFGF protein expression levels in SW1353 and SW135R cells were analyzed by Western blot. α-Tubulin was used as a loading control. Western blot shows dose-dependent effects of Dox on the expression of bFGF in SW1353 and SW1353R cells at indicated dose for 24 h. α-Tubulin was used as a loading control. (D) The bFGF levels of cell lysate from SW1353 and JJ012 cells were analyzed by Western blot (left panel). Serum-starved SW1353 and JJ012 cells were exposed to indicated doses of Dox for 24 h and assayed for survival by MTT (right panel).

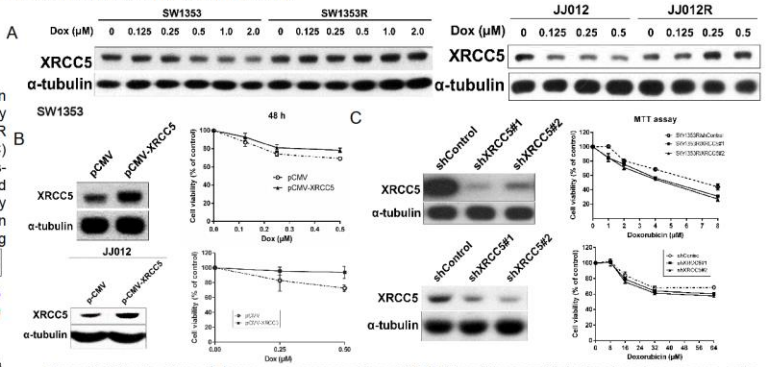

Figure 5. Effects of knockdown or overexpression of XRCC5 on Dox sensitivity in chondrosarcoma cells.
(A) SW1353 cells were treated with indicated concentration of Dox (0-2 μM) for 24 h and the expression levels of XRCC5 were examined by Western blot. The data show the mean expressed as mean ± SEM of at least 6 independent experiments. * P < 0.05, compared with the control (0 μM). JJ012 cells were treated with indicated concentration of Dox (0-0.5 μM) for 24 h and the expression levels of XRCC5 were examined by Western blot. α-Tubulin was used as a loading control. The data show the mean expressed as mean ± SEM of at least 4 independent experiments. * P < 0.05, compared with the control (0 μM). (B) Overexpression of XRCC5 induces Dox resistance in cells by Western blot. α-Tubulin was used as a loading control. Cells were exposed to increasing concentrations of Dox for 48 h and subsequently evaluated by MTT assay. * P < 0.05 compared with pCMV/pCMV-XRCC5.(up panel : SW1353;down panel : JJ012).(C) The protein levels of XRCC5 in shControl and shXRCC5 were examined by Western blot. α-Tubulin was used as a loading control. Cells were exposed to increasing concentrations of Dox for 24 h and subsequently evaluated by MTT assay. The percentage of cell viability is shown relative to untreated controls. *P<0.05 compared with shXRCC5/shControl.(up panel : SW1353R;down panel : JJ012R)

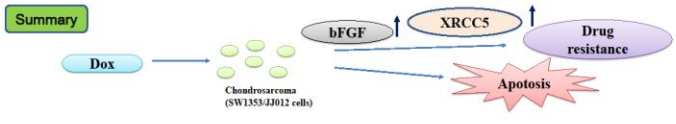

國立嘉義大學
National Chiayi University

Investigate the biological activities of astaxanthin-loaded liposomes in bone cells.

Chu-Wen Shao[1#] , Chi-Hsiang Lai[1] and Hsin-I Chang[1]

[1] Department of Biochemical Science and Technology, National Chia Yi University, No 300, Syuefu Rd, Chiayi City 60004, Taiwan
[#]corresponding Author

ABSTRACT

Astaxanthin, a xanthophyll carotenoid commonly found in Haematococcus pluvialis and seafood. Astaxanthin is regarded as the strongest antioxidant in nature. The anti-oxidative property is over 100 times more efficient than vitamin E or vitamin C. Due to its super anti-oxidative ability, Astaxanthin has been widely applied as a human nutraceutical supplement for healthy benefit. Previous studies have reported that astaxanthin possesses significant pharmacological properties, including antioxidant, anti-inflammatory, and antitumor effects. In order to enhance the bioavailability of astaxanthin, we used soybean phosphatidylcholine to encapsulate astaxanthin for liposomal formation. Thus, this study used liposomes as drug carrier for astaxanthin to assess the potential in bone cells.

At first, we run HPLC to analyze the astaxanthin content in ultrasonic extract of shrimp shells. The ultrasonic extraction of shrimp shells with 99% ethanol solution presented higher astaxanthin content than the one extracted with 50% ethanol solution, and hence we selected the ultrasonic extraction of shrimp shells with 99% ethanol solution (99% astaxanthin extracts) for the further experiments. Next, we tested the antioxidant capacity of astaxanthin extracts by DPPH and ABTS assays, and found that its free radical scavenging rate is over 80% at the concentration of 1 μg/ml. In vitro, we used murine microphage cell line- RAW 264.7 and mouse osteoblast-like cells- 7F2 to test cell viabilities by MTT assay, liposomal formation can reduce the cytotoxicity of astaxanthin in cells. Furthermore, we tested the anti-inflammatory activities and scavenging intracellular ROS abilities by using Nitric Oxide and DCFDA staining assay in LPS-induced Raw 264.7 cells. So far, astaxanthin-loaded liposomes showed dose dependently anti-inflammatory effect and also reduced ROS level on LPS-induced RAW 264.7 cells. We determined the physical properties of astaxanthin-loaded liposomes by particle size, encapsulation efficiency and polydispersity index. The results revealed that the particle sizes of asta-loaded liposomes with various concentrations exhibited mean diameters in the range from 109 to 134 nm and had a narrow PDI value but increased in a dose-dependent manner. As expected , liposomes loaded with a high concentration of astaxanthin (1.02 μg/ml) showed a decline in entrapment efficiency from 89% to 29%. Furthermore, liposomes can be uptaken by 7F2 osteoblasts after 4 hours of incubation. In addition, alizarin red staining and calcium content measurement showed that there was no significant difference in calcium deposition for the 7F2 osteoblasts treated with 0.05 μg/ ml of asta-loaded liposomes in comparison with the cells treated with drug-free liposomes and MM group.

In conclusion, we confirmed the presence of astaxanthin in the ultrasonic extract of shrimp shells and that extract exhibited powerful anti-oxidant potential. Liposomal formulation can reduce the cell cytotoxicity of astaxanthin. Moreover, 0.05 μg/ ml of asta-loaded liposomes may slightly suppress ALP activity and mineralization level in 7F2 osteoblasts but show anti-inflammatory effect and reduced ROS expression in RAW264.7 macrophages. Therefore, we demonstrated that astaxanthin extract may be able to protect bone against oxidative stress, inflammation and bone loss.

Experimental design

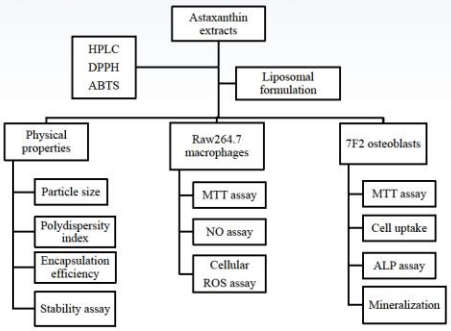

RESULTS

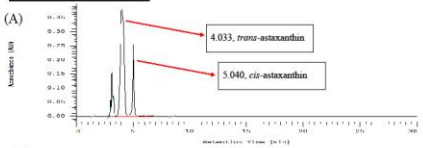

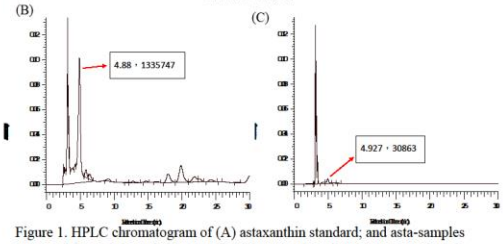

Figure 1. HPLC chromatogram of (A) astaxanthin standard; and asta-samples extracted from shrimp shell wastes by (B) 99% ethanol and (C) 50% ethanol.

Table 1. The concentration of astaxanthin in the extracts of shrimp shell wastes

shrimp shells extracted by ethanol solution	99%	50%
Peak area	1335747	30863
astaxanthin concentration (μg/ml)	10.229	0.889

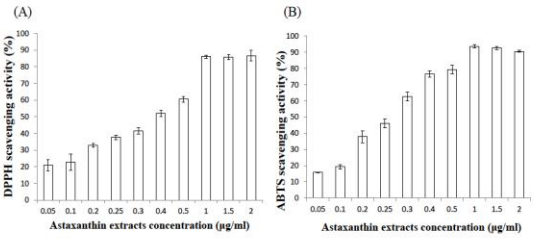

Figure 2. (A) The antioxidant ability of astaxanthin extracts measured by DPPH assay. (B) The ABTS radical scavenging activity of astaxanthin extracts.

Table 2. Physical parameters of liposomal formulation

Drug formulation	Particle size (nm)	PDI value	Entrapment Efficiency (%)
Empty liposomes	134.35± 3.48	0.1502± 0.014	--
asta-liposomes 0.05 μg/ml	123.40± 1.83	0.1409± 0.027	89.001± 0.41
asta-liposomes 0.25 μg/ml	123.40± 3.11	0.1474± 0.040	53.905± 1.76
asta-liposomes 0.51 μg/ml	109.68± 2.81	0.1661± 0.013	43.857± 0.81
asta-liposomes 1.02 μg/ml	127.78± 3.44	0.1701± 0.032	29.399± 0.91

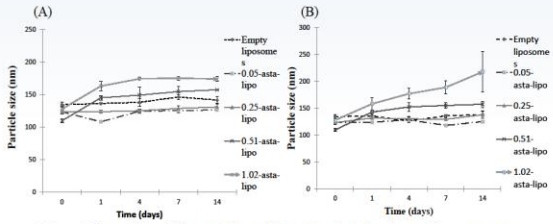

Figure 4. The stability of liposomal formulations. Asta-loaded and empty liposomes were stored at 4℃ (A) and 37℃ (B) in DMEM containing 10% CCS and incubated 1, 4, 7, 14 days.

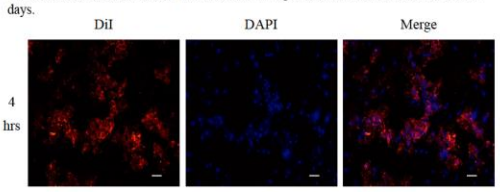

Figure 5. *In vitro* uptake of DiI-labeled liposomes in 7F2 osteoblasts for 4 hrs. measured by fluorescent microscopy. (×100 magnification, scale bar = 200 nm.)

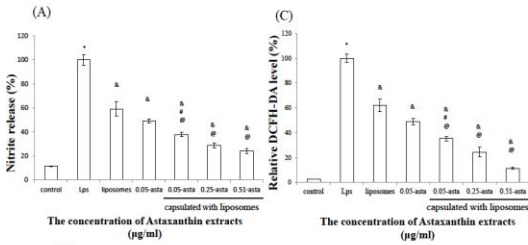

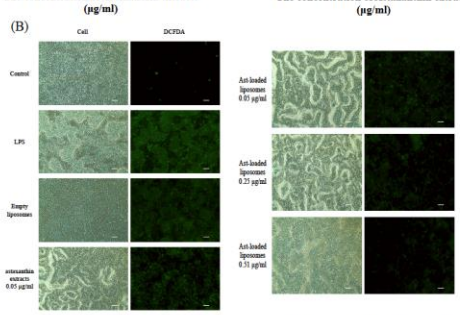

Figure 8. The effect of asta-loaded liposomes on nitrite (A) and intracellular ROS production (B,C) of LPS-induced Raw264.7 mouse macrophage cells. (* p<0.05 related to control, & p<0.05 related to LPS, @ p<0.05 related to cells treated empty liposomes, and # p<0.05 related to cells treated with 0.05 μg/ml astaxanthin extract.)

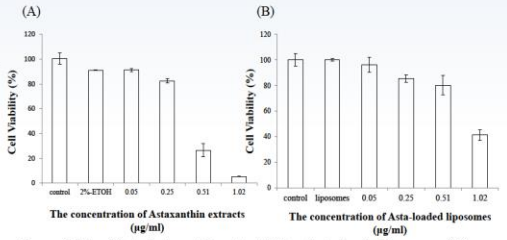

Figure 6. The effect of astaxanthin extract (A) and asta-loaded liposomes (B) on cell viability of Raw264.7 mouse macrophages.

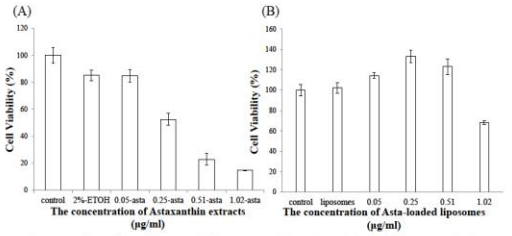

Figure 7. The effect of astaxanthin extracts (A) and asta-loaded liposomes (B) on cell viability of 7F2 osteoblast cells.

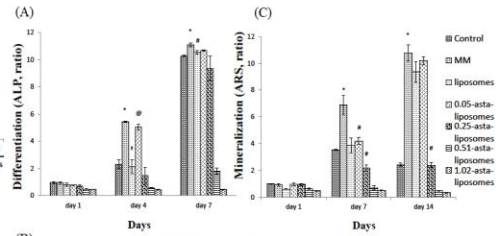

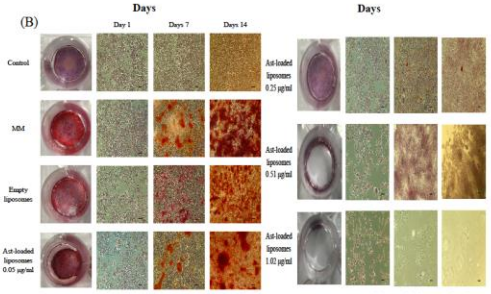

Figure 9. The effect of asta-loaded liposomes on 7F2 osteoblast differentiation (ALP production, A) and mineralization (B, C) . (* p<0.05 related to control group of the same day, # p<0.05 related to MM of the same day, @ p<0.05 related to empty liposomes treatment of the same day.)

Conclusion

- ☼ We found that ultrasonic extraction with 99% ethanol solution presented higher astaxanthin content than the one extracted with 50% ethanol solution.
- ☼ We confirmed that the astaxanthin extracts exhibited powerful anti-oxidant ability.
- ☼ *In vitro* experiments, liposomal formulation of astaxanthin extracts have a major influence on reducing the cytotoxicity of 7F2 osteoblasts and Raw264.7 macrophages and may have the potential to stimulate cell proliferation.
- ☼ Asta-loaded liposomes could protect Raw264.7 cells from LPS-induced oxidative stress by scavenging intracellular ROS and show anti-inflammatory activity through the inhibition of NO production.
- ☼ 0.05 μg/ml could be the best concentration of asta-loaded liposomes for remaining osteoblast differentiation and mineralization.
- ☼ Taken together, liposomal formulation of astaxanthin extracts have good potential to protect bone against oxidative stress, inflammation and bone loss.